

Protein molecular responses of field-collected oysters *Crassostrea hongkongensis* with greatly varying Cu and Zn body burdens

Yunlong Li^{a,b}, Wen-Xiong Wang^{b,c,*}

^a Division of Life Science and Hong Kong Branch of the Southern Marine Science and Engineering Guangdong Laboratory (Guangzhou), The Hong Kong University of Science and Technology, Kowloon, Hong Kong

^b School of Energy and Environment and State Key Laboratory of Marine Pollution, City University of Hong Kong, Kowloon, Hong Kong

^c Research Centre for the Oceans and Human Health, City University of Hong Kong Shenzhen Research Institute, Shenzhen, 518057, China

ARTICLE INFO

Keywords:

Hyper-accumulation
Oyster
Metals
Protein level
ROS clearance

ABSTRACT

The oyster *Crassostrea hongkongensis* is an ideal biomonitor due to its widespread distribution along the coast of Southern China and the ability to hyperaccumulate metals including Cu and Zn. In this study, we conducted the first investigation of the molecular responses to metal hyperaccumulation based on quantitative shotgun proteomics technique and genome information. Gill tissue of oysters collected from the uncontaminated environment (Site 1, 59.6 µg/g and 670 µg/g dry weight for Cu and Zn) displayed significant protein profile differentiation compared to those from a moderately contaminated (Site 2, 1,465 µg/g and 10,170 µg/g for Cu and Zn) and a severely contaminated environment (Site 3, 3,899 µg/g and 39,170 µg/g for Cu and Zn). There were 626 proteins identified to be differentially expressed at Site 3 but only 247 proteins at Site 2. Oysters from a moderately contaminated estuary (Site 2) displayed fewer effects as compared to oysters under severe contamination, with fluctuated small molecule metabolism and enhanced translation process. At Site 3, the induction of reactive oxygen species (ROS) was the main toxicity under the extremely high level of metal stress, which resulted in protein damage. Additionally, the impaired structure of cytoskeleton and modified membrane tracking process at Site 3 oysters led to the blockage or less efficient protein or macromolecule distribution within cells. Nonetheless, proteomic analysis in this study revealed that oysters could partly alleviate the adverse metal effects by boosting the translation process, enhancing the ability to recycle the misfolded proteins, and enhancing the potential to eliminate the excess ROS. Our study demonstrated an adaptive potential of oysters at the protein level to survive under conditions of metal hyper-accumulation.

1. Introduction

Estuaries in China face tremendous environmental challenges due to the rapid economic development and direct releases of industrial effluents. Metal pollution is one of the most common and predominant types of anthropogenic pollution, especially in the coastal and estuarine areas where industrialization is actively explored and developed. Meanwhile, estuaries are characterized by high biodiversity and biomass production. Previous studies found that the estuarine oysters *Crassostrea hongkongensis* accumulated trace metals up to 6.0 % of Zn (Li et al., 2020) and 2.6 % of Cu in their gill tissues (Weng and Wang, 2015) (normalized by dry weight). Due to their widespread distribution in the Southern China estuaries, *C. hongkongensis* is also an ideal bivalve as a biomonitor of metals. As a result of their severe contamination, blue oysters

containing extraordinarily high metal concentrations were firstly reported in 2011 in Jiulong River Estuary of China, and subsequently in other Southern China estuaries (Li et al., 2020; Wang et al., 2011; Weng et al., 2017; Weng and Wang, 2019).

A few studies tried to address why oysters survive despite the extremely high metal body burdens (mainly for Zn and Cu). Two strategies were generally adopted to facilitate the oysters *C. hongkongensis* to detoxify the trace metals at the subcellular levels. With increasing metal concentration, the proportion of Cu in the cellular debris and Zn in the metallothionein-like protein (MTLP) fractions increased simultaneously, indicating that oysters sequestered metals to detoxify the incoming metals (Wang et al., 2011; Yu et al., 2013). Tan et al. (2015) suggested that a large amount of Cu and Zn was associated with oxygen- and nitrogen-bound complexes in contaminated oysters but not the

* Corresponding author at: School of Energy and Environment and State Key Laboratory of Marine Pollution, City University of Hong Kong, Kowloon, Hong Kong.
E-mail address: wx.wang@cityu.edu.hk (W.-X. Wang).

<https://doi.org/10.1016/j.aquatox.2021.105749>

Received 24 September 2020; Received in revised form 27 December 2020; Accepted 11 January 2021

Available online 19 January 2021

0166-445X/© 2021 Elsevier B.V. All rights reserved.

sulfur-bound ones. Meanwhile, a similar mechanism was also documented through co-localization identification among elements at the subcellular imaging level (Weng et al., 2017). Time-series and spatial biomarker measurement provided some mechanistic insight into the responses of a few traditional chemicals in oysters *C. hongkongensis*, such as metallothionein, superoxide dismutase, and glycogen (Chan and Wang, 2019; Liu and Wang, 2016a, b, 2016c). The metabolomic study revealed changes of metabolites in oysters, indicating the disturbance of osmotic and energy regulation under metal stress (Ji et al., 2015). Chan and Wang (2018a) employed lipidomics to analyze the change of small molecules in oysters under Cu stress. More recently, Li et al. (2020) studied the differentiation in oysters stressed by different levels of metals and identified two putative transporters for Cu/Zn accumulation via RNA-sequencing (RNA-seq).

Protein, as the final functional biomacromolecule, needs to be further investigated since its expression level might not match the transcriptional profile. There are some steps in the process from RNA to protein, such as micro-RNA binding, N⁶-methyladenosine, and RNA splicing, which work as the post-transcriptional modifications. Such a reaction would cause the blockage of translation. The mRNA can be spliced and recombined into different proteins, although these proteins are from the same DNA sequence (Di et al., 2019). mRNA degradation or blockage of translation can occur when microRNA binds to target mRNA (O'Brien et al., 2018). Therefore, it is necessary to understand the phenotypic responses of oysters under stress conditions at the protein expression levels in addition to RNA-seq.

Proteomic tools are now widely used in the biological study, and permit us to obtain high throughput profiles at the protein level. The 2D-gel-electrophoresis-proteomics was firstly employed to analyze the expression patterns of proteins in oysters under different metal stress conditions. Significant changes in the proteome pattern were documented when oysters *C. hongkongensis* were grown in metal-rich environments (Liu and Wang, 2012; Luo et al., 2014; Xu et al., 2016). The other species of oyster *Crassostrea sikamea* has also been studied in their responses to metal pollution via 2D-gel-electrophoresis-proteomics (Lu et al., 2019b). Similarly, Muralidharan et al. (2012) demonstrated that proteomics is a promising approach to evaluate the effect of metals in Sydney rock oysters. However, these earlier studies were mostly based on the 2D-SDS-PAGE techniques with a limited number of proteins identified. Recently, isobaric tag for relative and absolute quantitation (iTRAQ) has become a powerful technique in proteomics, being able not only to identify a greater number of proteins but also precisely quantify relative abundances of protein among different samples. Meng et al. (2017b; and, 2018) analyzed the differentially expressed proteins in *Crassostrea gigas* under laboratory exposure conditions and demonstrated that Zn and Pb exposure caused respiration disruption. Other studies have also used iTRAQ to unravel the differential proteomic responses to salinity, thermal and virus exposure, and ocean acidification in bivalves (Dineshram et al., 2015; Li et al., 2019; Masood et al., 2016; Venkataraman et al., 2019; Zhang et al., 2015).

Nevertheless, laboratory-controlled exposure studies do not realistically reflect the exposure conditions and responses in the field environment, and most of these studies merely examined the response to a single factor. In this study, three populations of oysters *C. hongkongensis*, which grew naturally at different levels of metals in the estuaries across Southern China, were sampled and their patterns at the protein level were compared. The quantitative proteomics (iTRAQ) was first applied to observe the toxicity and response of oysters *C. hongkongensis* experiencing metal hyper-accumulation. Our study identified several new biomarkers of metal exposure and provided a more detailed mechanistic understanding of the systemic proteomic responses of oysters of field-collected oysters with very high Cu and Zn body burdens.

2. Materials and methods

2.1. Oyster collection

Oysters *C. hongkongensis* mainly distribute in the estuarine environment in Southern China and accumulate metals in contaminated environments, at (dry weight) tissue concentrations as high as 24,000 µg/g for Zn and 14,000 µg/g for Cu (Lu et al., 2017; Wang et al., 2011). In the present study, *C. hongkongensis* (about 2-year-old, shell length 80–120 mm) growing naturally at three different levels of trace metals were collected during the low tide (height < 50 cm). Fig. 1A shows the locations of the three sampling sites. Site 1 (21°26'N, 109°18'E) was far away from the industrial region with the lowest Cu/Zn accumulation in *C. hongkongensis*, and could, therefore, be regarded as a relatively clean environment (Lu et al., 2017). Contaminated oysters were sampled near Xiamen (Site 2, 24°28'N, 117°54'E) along Jiulong River Estuary (a moderately contaminated system) and from Shantou (Site 3, 23°22'N, 116°34'E) along Rong River Estuary (a severely contaminated system). There was little difference in the temperature and salinity among the three sampling sites when we sampled (Fig. 1A). Previous studies documented that these two estuaries were contaminated with metals, especially for Cu and Zn (Tan et al., 2015; Wang et al., 2011; Weng and Wang, 2014). Fifty-four individuals of oysters from each station were dissected immediately after sampling. The ultra-pure water (MilliQ water with 18.2 MΩ-cm, Millipore) was used to remove some impurities on the oyster shell surface. Then, gills were separated from the soft tissue and cut into pieces for further analysis, including metal concentration and proteomics. To prevent the proteins from degradation, samples were immediately frozen in liquid nitrogen and stored at -80 °C until needed.

As described earlier, the cytochrome oxidase subunit I (COI) gene was used as a molecular marker for taxonomic identification among oysters *Crassostrea* species (Wang and Guo, 2008). Universal and specific primers were applied to obtain the COI fragment as shown below. COI forward: GGGACTACCCCTGAATTTAAGCAT, COChk387r: GGAGTAAGTGATAAGGGTGGATAG. DNA gel electrophoresis indicated the oysters sampled in this study all belonged to *Crassostrea hongkongensis* (Fig. S1).

2.2. Metal concentrations in the gills

After freeze-dried at -50 °C (SCIENTZ, China), the dry weights of samples were measured. The dried samples (about 100 mg) were then mixed with 3 mL 65 % nitric acid (Sigma-Aldrich, USA) in each 15 mL tube (Falcon, USA) at 80 °C for 12 h to digest fully. The digested gill samples were diluted with Milli-Q water and then quantified by inductively coupled plasma mass spectrometry (ICP-MS, NexION 300X, PerkinElmer, USA). In the present study, trace metals (Cu and Zn) in certified reference materials SRM 1566b was also measured in the same manner, with acceptable recoveries between 90 % and 120 %. For quality control (QC), a mixed solution with 10 µg/L multi-elements was determined after the standard curve and every 10 samples to quality-assurance purposes. The deviations between the known value and measured value were all less than 20 %, indicating the reliable results obtained in each analytic run.

2.3. Protein extraction and quantification

About 0.1 g sample was placed in the Lysis buffer 3 (pH = 8.5, containing 8 M Urea, 40 mM Tris-HCl with 1 mM PMSF, 2 mM EDTA and 10 mM DTT). After homogenizing in TissueLyser with two 5 mm beads at 50 Hz for 2 min, the mixture was centrifuged (25,000 g, 4 °C, 20 min) to obtain the supernatant which was transferred to a new tube. Dithiothreitol (DTT, 10 mM final concentration) was added to the supernatant to reduce the disulfide bonds in proteins. After 1 h incubation at 56 °C, the mixture was alkylated in iodoacetamide (IAM, 55 mM final concentration) under dark at 25 °C for 45 min. Finally, the protein solution

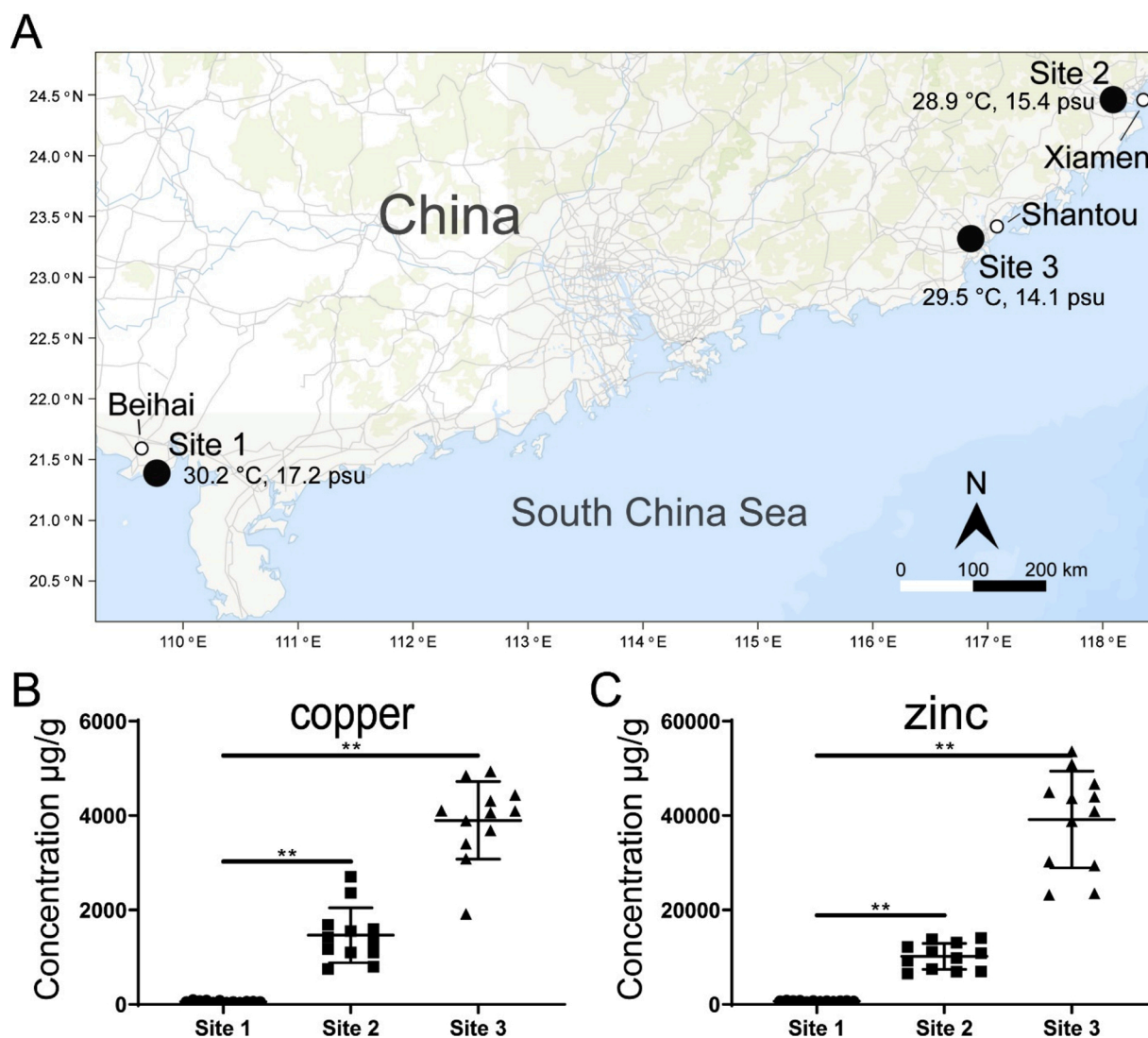


Fig. 1. The three sampling sites in Southern China (A) and the accumulated concentrations of trace metals (Cu and Zn) in the gills of oysters (12 individuals in each site) from three sites (B, C). The temperature and salinity of seawater at sites were presented in the map. ** indicates the significance (Sig. < 0.001) in SPSS version 22.0.

was obtained after centrifugation (25,000 g, 4 °C, 20 min). Bradford assay and SDS-PAGE were used to measure the concentration and quality of protein extracted. Only high-quality proteins (the amount of total protein > 1 mg, clear bands, and good repeatability) were kept for further experiments.

2.4. iTRAQ labeling and peptide fractionation

Given the potential individual variation in the field sample, the pooled sample can provide the average state of protein expression and reduce the variation across individuals with acceptable deviation (Kaur et al., 2012; Liao et al., 2008; Song et al., 2008; Yan et al., 2014). In the present study, pooled samples were adopted to conduct a quantitative proteome. 18 replicated oyster individuals were collected from each site (54 individuals in total for the three sites) for the proteomic analysis. Protein homogenates of six individual oysters were pooled together to form one biological replicate, thus there were three biological replicates for each population (i.e., a total of 18 individuals, $n = 3$).

Triethylammonium bicarbonate (TEAB, 100 mM) was used to dilute the pooled proteins (100 µg). After Trypsin Gold (Promega, USA) digestion with a weight ratio (trypsin: protein = 1:40) at 37 °C for 16 h, the obtained peptides were desalted with a Strata X C18 column

(Phenomenex, USA) and dried under vacuum. The peptides dissolved in 30 µL TEAB (0.5 M) were labeled with isobaric tags (iTRAQ, Applied Biosystems, USA). Samples were then pooled together, followed by desalting and vacuum-drying. Nine analyzed protein samples were separated into three runs. In each run, 114, 115, and 117 were labelled for Site 1, Site 2, and Site 3, respectively.

The reconstituted peptides in solution A (5% acetonitrile and 95% H₂O, pH = 9.8) were separated using LC-20AB High-Performance Liquid Chromatography (HPLC) Pump system (Shimadzu, Japan) at 1 mL/min flow rate, i.e., Strong Cation Exchange fractionation (waters BEH C18 4.6 × 250 mm, 5 µm). A set of gradient buffer B (5% H₂O and 95% acetonitrile, pH = 9.8) was used to conduct the process: 5% buffer B for 10 min, 5–35% buffer B for 40 min, and 35–95% buffer B for 1 min. Twenty collected fractions were desalted and vacuum-dried again.

2.5. LC-MS/MS analysis

Each fraction was reconstituted in solution C (2% acetonitrile and 0.1% formic acid in H₂O). The supernatant obtained after centrifugation (20,000 g, 4 °C, 10 min) was separated by the analytical C18 column using the LC-20AD nano-HPLC instrument (Shimadzu, Japan) and then analyzed by TripleTOF 5600 System (SCIEX, USA) controlled with

Analyst 1.6 (SCIEX, USA). Solution D (2 % H₂O and 0.1 % formic acid in acetonitrile) with different concentrations with 300 nL/min flow rate was applied to run: 8–35 % for the initial 35 min, 60 % for 5 min, 80 % for 5 min, and a final 5 % for 10 min 6 s. The whole data acquisition was performed in high sensitivity mode under the following MS conditions: ion spray voltage 2300 V, curtain gas of 30, nebulizer gas of 15, and interface heater temperature of 150 °C. As many as 30 product-ion scans with 2+ to 5+ charge states above 120 counts/s in MS1 were collected for MS2. Meanwhile, the collision energy was calibrated by precursor ions due to collision-induced dissociation.

2.6. Bioinformatic analysis

Raw data generated from LC–MS/MS was converted into mzML format via AB SCIEX MS Data Converter. In this study, Trans Proteomics Pipeline (TPP) was employed for the following MS data processing (Deutsch et al., 2010). Specifically, Comet (Eng et al., 2013) was applied in MS/MS database search against the 29,482 proteins from *Crassostrea hongkongensis* genome (unpublished data from Dr. Ziniu Yu in South China Sea Institute of Oceanology, Chinese Academy of Sciences). The parameters in Comet were set as default except peptide_mass_tolerance = 50 ppm, mass_type = monoisotopic masses, isotope_error = 0, variable_mod02 = 304.2022 Y 0 3 -1 0 0, fragment_bin_tol = 0.1, fragment_bin_offset = 0.0, theoretical_fragment_ions = 0, clear_mz_range = 112.5 121.5, add_Nterm_peptide = 304.2022, add_C_cysteine = 57.021464, add_K_lysine = 304.2022. During the process, the decoy database (randomized peptides) was adapted to evaluate the error rate. The reliable protein library was constructed from PeptideProphet and ProteinProphet (Nesvizhskii et al., 2003), for peptide and protein validation, respectively. The cut-off values of both two were set as 1 % false discovery rate. The isotope intensity of labeled peptides was quantified by Libra in TPP. The identification of differentially expressed proteins (DEPs) was based on the method reported by Kammers et al. (2015). Only proteins that could be quantified in all three runs were selected in the following analysis. The criteria for DEPs was fold-change < 0.87 or fold-change > 1.15, with *q*-value < 0.05 in ordinary t-statistical analysis.

Genes obtained from the genome of *C. hongkongensis* were annotated against databases including NCBI non-redundant and SwissProt, using blast + version 2.7.14 (Camacho et al., 2009). Gene Ontology (GO) information of each gene was acquired against the idmapping file with the help of python, as described by Li et al. (2020). Kyoto Encyclopedia of Genes and Genomes (KEGG) annotation of genes was conducted by an online tool, BlastKOALA (Kanehisa et al., 2016). GOseq (R package) was applied to determine whether the category of proteins (both GO and KEGG) were significantly enriched (Young et al., 2010), based on the hypergeometric test. At the result of Gene Ontology, only terms related to molecular function were presented in this study.

2.7. Real-Time PCR (RT-PCR) analysis

In addition to iTRAQ analysis and metal concentration determination, the gill tissues were also used for RNA extraction. Total RNA was extracted from gill powders ground in liquid nitrogen by RNeasy® Mini Kit (QIAGEN, Germany). The quality (RNA integrity number, RIN) and yield of RNA were examined by Agilent 2100 (Agilent, USA) and Nanodrop (Thermo Fisher). The process of RT-PCR detection was conducted as the previous study (Li et al., 2020). The relative gene expression was calculated via the $2^{-\Delta\Delta Ct}$ method, with EF-1 α as the internal reference gene. For each gene, three replicates from each population were randomly selected to conduct the RT-PCR as the pooling strategy in protein extraction. All the primers are shown in Table S1.

2.8. Statistical analysis

One-way ANOVA in SPSS 22.0 was applied to test the difference of metals between contaminated sites and control. The relationship

between protein expression from iTRAQ and gene expression from RT-PCR was assessed by the Pearson correlation in GraphPad 8.0. Other statistical analyses, including protein identification, differential expression, and functional enrichment, were carried out with the corresponded software mentioned before.

3. Results and discussion

3.1. Accumulation of trace metals

Previous research reported that there was little or only slight ecological risk from organic pollutants at all three sampling sites (Gu et al., 2020; Han and Currell, 2017; Kaiser et al., 2015; Tian et al., 2015). Polycyclic aromatic hydrocarbons (PAHs) were taken as example since they were relatively well-studied. The concentration of PAHs in the sediment of those three sites was below the effects range-low value (4, 022 ng/g, Long et al., 1995), Site 1: 24 ~ 647 ng/g (Kaiser et al., 2015), Site 2: 280 ~ 1,206.8 ng/g (Tian et al., 2008), Site 3: 46 ~ 1,665.2 ng/g (Gu et al., 2020). Nonetheless, these two contaminated environments (Site 2 and Site 3) were facing metal stress due to the effluents (Qiao et al., 2013; Xu et al., 2020). Furthermore, oysters *C. hongkongensis* are well-known for the ability to hyper-accumulate Cu and Zn, and for being bioindicators of metal contamination (Lu et al., 2017, 2019a; Pan and Wang, 2012; Tan et al., 2015; Weng et al., 2017; Wang et al., 2011). Therefore, we assumed oysters from Site 2 and Site 3 were under metal contamination (mainly for Cu and Zn) but no other pollutants.

Gill of oyster serves as the first interface between water and the internal environment and stores around 20 % of the whole tissue metals (mainly Cu and Zn) (Wang et al., 2011; Weng and Wang, 2015). In addition, the gill is the main metal uptake site so that metal concentrations in gills generally tend to be higher than in whole tissue (Liu and Wang, 2016b; Wang et al., 2011). Cu and Zn were considered as the main contaminants in our study, with gradient change among the three stations (Fig. 1B and 1C). For Cu, the highest concentration in gill tissue was at Site 3 (3,899 μ g/g), followed by Site 2 (1,465 μ g/g), and the lowest one at Site 1 (59.6 μ g/g). Similarly, Zn concentration in gill tissue also differed considerably among the three stations (670 μ g/g, 10,170 μ g/g, and 39,170 μ g/g for Site 1, Site 2, and Site 3, respectively). Meta-analysis and modeling studies showed that the baselines of Cu and Zn were only 34.5 and 340 μ g/g (Lu et al., 2019a). In this study, the concentration in the gill of oyster from Site 1 was slightly higher than that of baseline. On the other hand, up to 65-fold higher Cu and 58-fold higher Zn at Site 3, and up to 24-fold higher Cu and 15-fold higher Zn at Site 2, were observed as compared to those from Site 1. To rank the sites according to their metal concentrations, Site 2 was therefore defined as moderately metal contaminations whereas Site 3 was defined as severely metal contamination. Based on the earlier RNA-seq results that Cu and Zn overwhelmed the Cd effect (Li et al., 2020), we mainly focused on the potential roles of Cu and Zn in this study.

3.2. Proteome analysis

There were at least 350,000 spectra generated from TripleTOF 5600 system in each run. Overall, more than 3200 proteins were identified under the filtration strategy mentioned before (peptide_error_rate < 0.01, protein_error_rate < 0.01, and at least two unique peptides matched), 3245 in the first run, 3256 in the second run, 3280 in the third run. Among these, 2589 proteins were detected in all three runs, which then became the targets in our downstream analysis (Fig. S2A).

The protein expression was quantified based on the ion intensity labeling, which was used to determine whether there were different patterns among oysters under metal contamination, from the two metal contaminated sites (Site 2 & 3) vs. the uncontaminated site (Site 1). Compared to oysters with the lowest metal accumulation and from a relatively clean environment (Site 1), the protein profile showed distinct characteristics. The number of differentially expressed proteins (DEPs)

could reflect the proteomic response to metal exposure to some extent. More DEPs were detected at Site 3 (626 proteins, Fig. 2), and 247 proteins (about 44 %) were defined as differential expression at Site 2. There was a positive trend between the number of DEPs and the metal levels in oysters. The expression and annotation information of proteins are summarized in Table S2. Also, 92 proteins showed the same regulated patterns at both Site 2 and Site 3 oysters (14 upregulated and 78 downregulated, Fig. S2B). The results of RT-PCR similarly indicated a positive correlation between RNA and protein level (Fig. S3), although there may be some post-transcriptional modification that could affect the protein expression.

Similar to the numbers of DEPs at Site 2 and Site 3, the number of altered functions showed a positive correlation with the level of metal stress. There were 14 pathways enriched at both Site 2 and Site 3, and part of them were shown in Fig. 3A (labelled by “#”). Some of these showed similar regulation, including the “Ribosome”, “Exosome” and “Arginine and proline metabolism” pathway.

The Cu and Zn concentrations at Site 2 were about 40 % and 25 % of those at Site 3. The lower differential protein expression response observed at Site 2 compared to Site 3 indicated that oyster *C. hongkongensis* owned a certain ability to cope with different metal stress according to the different metal levels experienced. At Site 3, more metal toxicity for oysters was exhibited than that at Site 2. And more responses were observed at Site 3 in the meantime. Thus, the strategies of oysters surviving from severe metal contamination caught our attention.

3.3. Metal toxicity at the molecular level

3.3.1. Structural reorganization

Excess metals may cause stress on cell structural components. A previous study employing RNA-seq revealed that cytoskeletal components were the targets under severe metal contamination in oysters (Li et al., 2020). Proteomics could be a better tool to study the status of structural components under metal contamination. “Cytoskeleton proteins” was enriched significantly at Site 3, with 24 DEPs. Fig. 3B and Fig. 4A shows that most DEPs (30 out of 34 proteins) in the structural related functions belonged to downregulated proteins. There was only a 40 % decline of cofilin at both contaminated sites (Table S2). A lower abundance of filamin was detected at Site 2 (0.71-fold) and Site 3 (0.59-fold) compared to that at Site 1. The other downregulated proteins included dynein heavy chains, myosin heavy chain, spectrin, ankyrin, and tektin-3. The decreased expression of filamin (FLNA) and spectrin beta (SPTB) was also observed at the mRNA level by RT-PCR (Fig. 5A

and B).

The integrity of cytoskeleton guarantees the cells work well, including cell frame and cell mobility (Mateer et al., 2003). In Sydney rock oysters, a lower abundance of cytoskeleton proteins was caused by the exposure to Cu and Zn instead of Cd and Pb (Thompson et al., 2012). The reorganization of cytoskeleton in bivalves was a typical response to environmental changes such as ocean acidification, salinity and metal exposure (Luo et al., 2014; Su et al., 2018; Thompson et al., 2012; Xiao et al., 2018; Zhao et al., 2012). In this regard, the KEGG enrichment result also indicated that “Focal adhesion” was subdued (Fig. 3B), with most of the related proteins (14 of 15) downregulated, which was closely associated with the signal transduction across cell.

In general, the structural reorganization was ascribed to the hyper-accumulation of Cu and Zn in oysters, leading to the suppression of signal transduction, cell proliferation, and intracellular homeostasis. The rearrangement of cytoskeleton (mainly for disruption) could be developed as a new marker to identify whether oysters were under severe metal contamination.

3.3.2. Protein processing and secretion

Before the protein functions at a target, it needs to be processed by translation in the ribosome, modification in the endoplasmic reticulum (ER), and transport across the cell membrane by the vesicle. The pathway “Protein processing in endoplasmic reticulum” was expressed significantly and differently in oysters from severely contaminated estuary (Site 3). Only the correctly folded proteins are likely to be secreted by the cell, and Site 3 oysters displayed a much lower abundance of proteins participating in the correctly folded process (Fig. 6).

Ribosome-binding protein 1 (p180) was identified as having ribosome binding activity, which is required to initiate the translation process at the ribosome from mRNA to polypeptides. Suppressed activity (0.81-fold) of p180 in oysters from Site 3 was detected by iTRAQ. Afterwards, the newly translated polypeptides need glycosylation at the N-terminus of asparagine by the oligosaccharyltransferase complex (OST), which is part of the ribosome anchor, before entering the ER. The dysfunction of OST was evident based on the decreased abundance of its two subunits, dolichyl-diphosphooligosaccharide-protein glycosyltransferase subunit STT3A (STT3A, 0.83-fold) and subunit 48 kDa (WBP1, 0.78-fold). The nascent polypeptides are then transported into the ER via translocon, a multi-subunit membrane protein complex (Pfeffer et al., 2015). In this study, as one key component of the translocon, the protein transport protein Sec61 subunit alpha (Sec61) was expressed 30 % less at Site 3 compared to Site 1. These three proteins are located on the surface of ER membrane, playing key roles in the initiation of protein folding process in ER. Many enzymes are also involved in the correct protein folding with ER, among which calnexin (CANX) acts as a chaperone to allow only the correctly folded proteins to be secreted out of the ER. In this study, metal stress led to a 17 % lower activity of CANX, which might hinder correct protein folding or result in protein misfolding. In addition, transport protein Sec24B (Sec24) was less expressed (18 % lower), indicating that the secretion of proteins might also be suppressed.

In addition to the endoplasmic reticulum damage, a less activity of protein secretion and transportation across cell resulted from excess metal accumulation. Notably, hyper-accumulation of metals induced similar patterns in membrane related proteins as those of cytoskeletal elements. The KEGG enrichment indicated that “Membrane trafficking” was significantly altered in oysters with the highest metal body burden. Of the 66 DEPs belonging to “Membrane trafficking” at Site 3, 61 proteins were observed with lower abundance compared to Site 1 (Figs. 3B and 4B). The transport of macromolecule (such as proteins, lipids, other substances) relied on membrane trafficking, which is closely associated with signal transduction, endocytosis, and exocytosis (Ceresa and Schmid, 2000; Faini et al., 2013; Herrmann and Spang, 2015). The downregulation of elements located in the cell membrane would induce blockage or less efficient protein secretion and signal transduction, thus

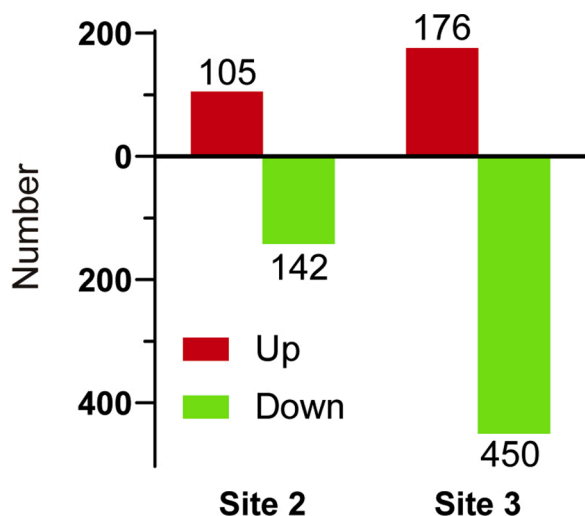


Fig. 2. The number of differentially expressed proteins at Site 2 and Site 3 compared to Site 1 oysters.

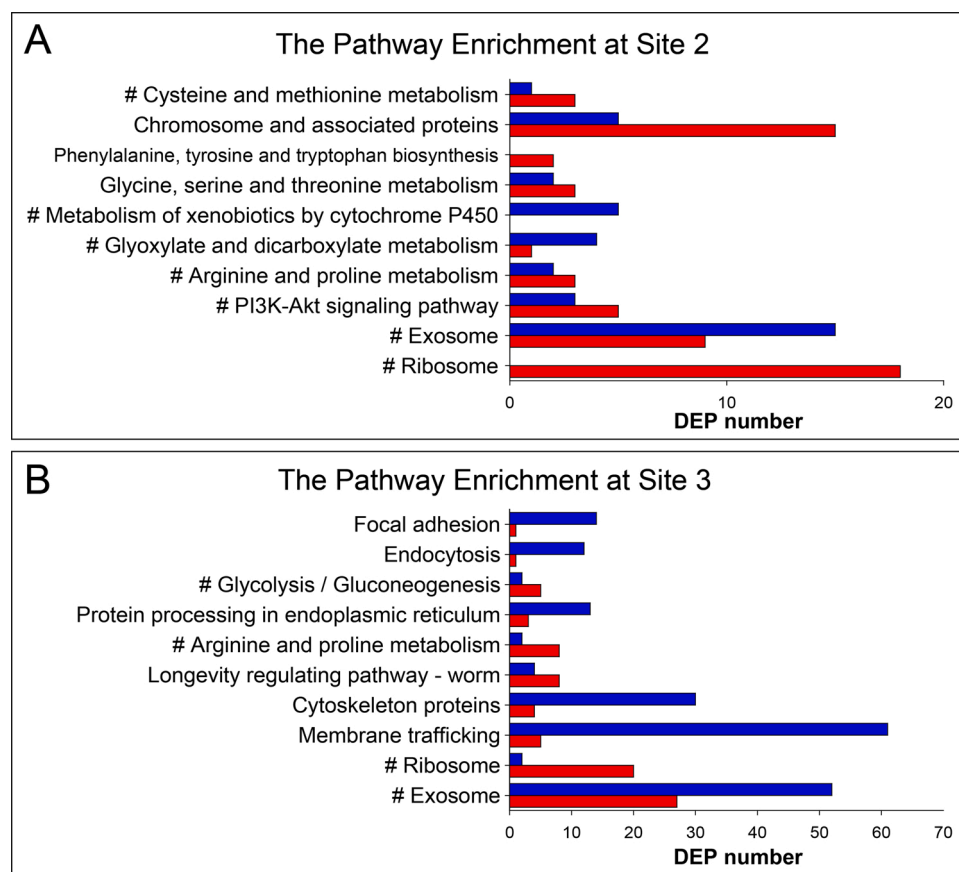


Fig. 3. The KEGG pathway enrichment analysis of DEPs at Site 2 (A) and Site 3 (B) (over_represented_FDR < 0.05). Only selected pathways are shown in the figure, while all pathways are shown in Table S3 (Site 2) and Table S4 (Site 3). “#” means that pathways were highlighted at both sites. Red bar signifies upregulated proteins whereas blue bar signifies downregulated proteins.

affecting the regular activity of cells (Cho and Stahelin, 2005). Similarly, hyposaline conditions caused the downregulation of proteins in vesicle transport in Pacific oyster as revealed by iTRAQ (Li et al., 2019). Transportation across organelles may also be affected. For example, protein transport protein Sec61 (Sec61) plays a crucial role in importing polypeptides into the ER. The lower expression of Sec61 subunit alpha (0.70-fold at Site 3) might lead to the reduction of protein synthesis. In addition, another protein Sec24, which is responsible for the protein secretion, was suppressed at Site 3.24

3.3.3. Possible reason for dysfunction

In this study, 450 downregulated proteins were identified at Site 3, and only 176 proteins were upregulated. The disruption of proteins, including the cytoskeleton elements, might be attributed to the excess of accumulated metals directly or indirectly. The excess Cu and Zn might substitute the original binding ions in proteins, thus causing the inactivation of proteins (Barber-Zucker et al., 2017). A total of 1,389 proteins were observed with metal ion binding activity according to the GO annotation of the encoded proteins in the *Crassostrea hongkongensis* genome. There were 267 proteins identified by iTRAQ that were shared among all three populations, accounting for 19.2 % of the metal ion binding proteins. However, there were only 66 metal ion binding proteins with lower abundance under metal contamination, which was only 14.7 % of 450 downregulated proteins. Therefore, based on our bioinformatic analysis, the hyper-accumulated Cu and Zn in oyster did not significantly impact the metal ion binding proteins, indicating that the dysfunction of proteins is unlikely to be due to the replacement of binding ions.

On the other hand, metal accumulation (Cu and Zn) is likely to affect the integrity of proteins indirectly via inducing the production of

reactive oxygen species (ROS) (Abdal Dayem et al., 2017; Auten and Davis, 2009; Lin et al., 2019; Stadtman and Levine, 2000; Xu et al., 2017). ROS includes superoxide (O_2^-), hydroxyl ($\cdot OH$), as well as hydrogen peroxide (H_2O_2). Although ROS are also produced via the electron transfer chain in the respiration process (Murphy, 2009), the exogenous ROS from accumulated metal ions might increase the proportion of downregulated proteins, including cytoskeleton and membrane associated proteins (Figs. 7 and 8). When facing high levels of oxidative stress, organisms may elevate the related antioxidant enzymes to cope with the stress. Previous studies have revealed that several proteins with antioxidant activity can be used as indicators of the level of oxidative stress, including the superoxide dismutase (SOD), Alpha-crystallin B chain (CRYAB), catalase (CAT) and glutathione S-transferase (GST) (Katerji et al., 2019; Khalil, 2015; Marrocco et al., 2017; Xu et al., 2016). The iTRAQ results showed that there were higher abundances of these proteins in oysters from Site 3 (Table 1). Superoxide dismutase [Cu-Zn] (CuZnSOD) was expressed up to 2.10 times and the others (CAT, CRYAB and two GSTs) were 1.15 ~ 1.22 times higher at Site 3 compared to Site 1, which indicated the production of ROS from excess accumulated Cu and Zn. Furthermore, higher expressions of these antioxidant enzymes were detected at the mRNA level (Fig. 5D-H). Higher ROS production in oysters was found under excess metal stress (Chan and Wang, 2018b, 2019), which can target the proteins and affect the integrity of protein. Therefore, we speculated that the ROS was induced by excess metals and then further imposed damage on proteins, thus reducing the protein abundance and affecting some of the key compartments (cytoskeleton, membrane trafficking and ER).

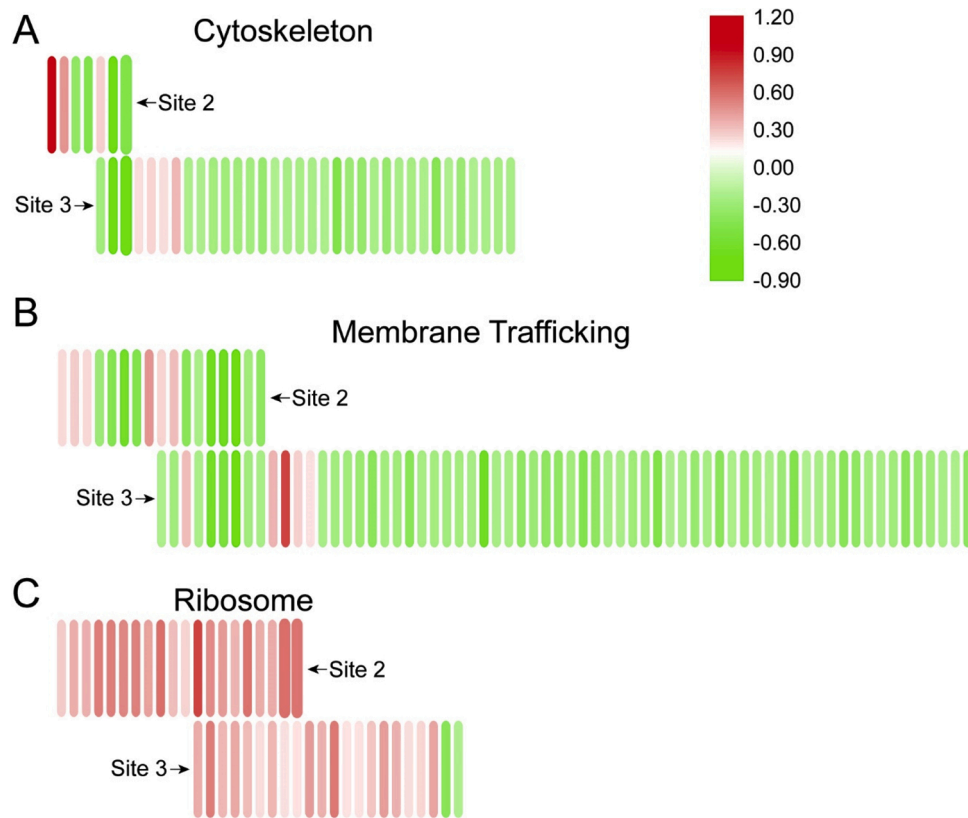


Fig. 4. The heatmap of proteins in “Cytoskeleton” (A), “Membrane Trafficking” (B), and “Ribosome” (C), with the mean change of 3 replicates. Red color signifies a higher abundance than control (Site 1) whereas green signifies lower. Heatmap graph was drawn by TTools (Chen et al., 2020).

3.4. Adaptive response and strategy under severe metal contamination

One of the most puzzling questions in oysters facing severe metal stress is their survival strategy. Oysters facing severe metal concentrations manage to survive and reproduce, suggesting that there are effective biochemical and molecular mechanisms that help to mitigate the adverse effects associated with this type of environmental stress. These mechanisms can be revealed by functional enrichment analysis.

3.4.1. Translation at the ribosome

Ribosomes serve as the sites for protein synthesis in eukaryotes, containing 40S and 60S subunits (de la Cruz et al., 2015). Based on the GO and KEGG enrichment analysis, the abundance of ribosome-associated proteins was significantly altered at both metal-contaminated sites, compared to Site 1. Remarkably, the bulk of DEPs annotated as ribosomal proteins were expressed more actively in oysters from contaminated sites (Site 2 and Site 3) as comparison to Site 1. Specifically, 20 of 22 DEPs at Site 3 and 18 of 18 DEPs at Site 2 were upregulated (Figs. 3 and 4C). In addition, 7 proteins (ribosomal protein S6, S16, S17, S24, L8, L19 and L21) were upregulated at both sites. Among them, S24 and L19 were selected to check the correlation between iTRAQ and RT-PCR, showing a positive relationship (Fig. 5J and K). Ribosomal proteins are indicators or biomarkers in bivalves exposed to metals including Pb, Zn, and Cd (Bao et al., 2016; Meng et al., 2017a; Thompson et al., 2012). Ribosome activity is closely correlated with the translation process. Increased expression of ribosomal proteins indicated the higher abundances of ribosome. In this study, higher translation activity was observed at both contaminated sites, indicating a significant role in helping oysters cope with metal stress. Given the disruption in protein processing in the ER and the suppression in protein transportation across cells, oysters might promote the compensatory system by increasing the abundance of ribosome associated proteins, thus promoting the translation process.

3.4.2. Degradation of misfolded proteins

High metal concentrations in the cell cause damage to protein synthesis. As mentioned before, the impairment of the ER might impede the process of correctly folding or result in the consequent protein misfolding. In addition, protein oxidation might occur due to higher ROS levels caused by excess metal ions. To maintain cellular homeostasis, oysters might enhance the ability to degrade misfolded proteins or damaged proteins (Fig. 6). In the present study, ER-associated degradation (ERAD) was enhanced under metal stress, with three proteins upregulated. The UV excision repair protein RAD23 homolog B-like (RAD23, 1.19-fold) is required for the degradation of proteins involved in ERAD (Wade and Auble, 2010). The other two proteins are members of the heat shock protein family and were over expressed by 22 % and 68 % at Site 3. They can bind with improperly folded proteins to proceed with ER-associated degradation (Sun and Brodsky, 2017; Yamamoto et al., 2014). With more misfolded proteins produced by excess metals, a higher abundance of RAD 23, HSP70 and CRYAB could ensure the degradation of these misfolded proteins by the proteasome without being secreted out of the cell (Fig. 5G and H). In Pacific oysters and in human, ERAD serves as a security guard to prevent the accumulation of misfolded protein induced by metals in the laboratory-controlled experiment (Adele et al., 2009; Meng et al., 2017b). In summary, elevated ERAD activity serves the purpose of degrading misfolded proteins (Fig. 6).

3.4.3. ROS clearance

Damage by metals is partly attributable to the ROS (Giarratano et al., 2010; Mesquita et al., 2019; Podgurskaya and Kavun, 2006), which is produced via the electron transfer chain in the respiration process (Murphy, 2009) mainly under the reaction of complex I, II, and III (Fig. 7). The other source of ROS is exogenous, e.g., Cu can produce ROS via Fenton-like reaction (Bejaoui et al., 2020; Klimova et al., 2019; Vranković, 2015) and Zn could induce ROS in cell (Lin et al., 2019). In

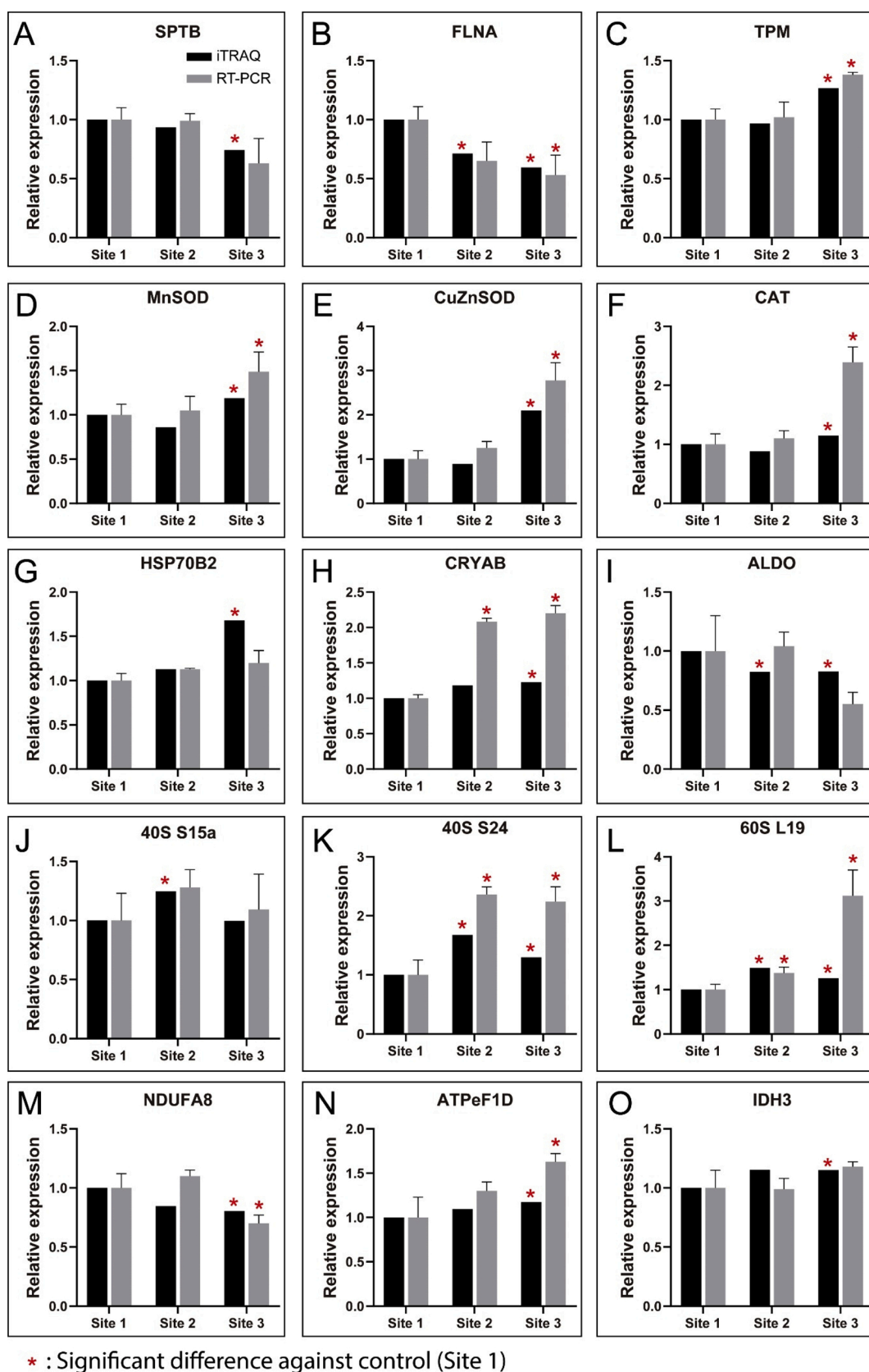


Fig. 5. The expression of 15 proteins by iTRAQ and expression of corresponding genes by RT-PCR. A: spectrin beta (SPTB), B: filamin A (FLNA), C: tropomyosin (TPM), D: superoxide dismutase [Mn] (MnSOD), E: superoxide dismutase [Cu-Zn] (CuZnSOD), F: catalase (CAT), G: heat shock protein 70 B2 (HSP70B2), H: alpha-crystallin B chain (CRYAB), I: fructose-bisphosphate aldolase (ALDO), J: 40S ribosomal protein S15a (40S S15a), K: 40S ribosomal protein S20 (40S S24), L: 60S ribosomal protein L19 (60S L19), M: NADH dehydrogenase [ubiquinone] 1 alpha subcomplex subunit 8 (NUDFA8), N: ATPeF1D; F-type H⁺-transporting ATPase subunit delta (ATPeF10), O: isocitrate dehydrogenase (IDH3).

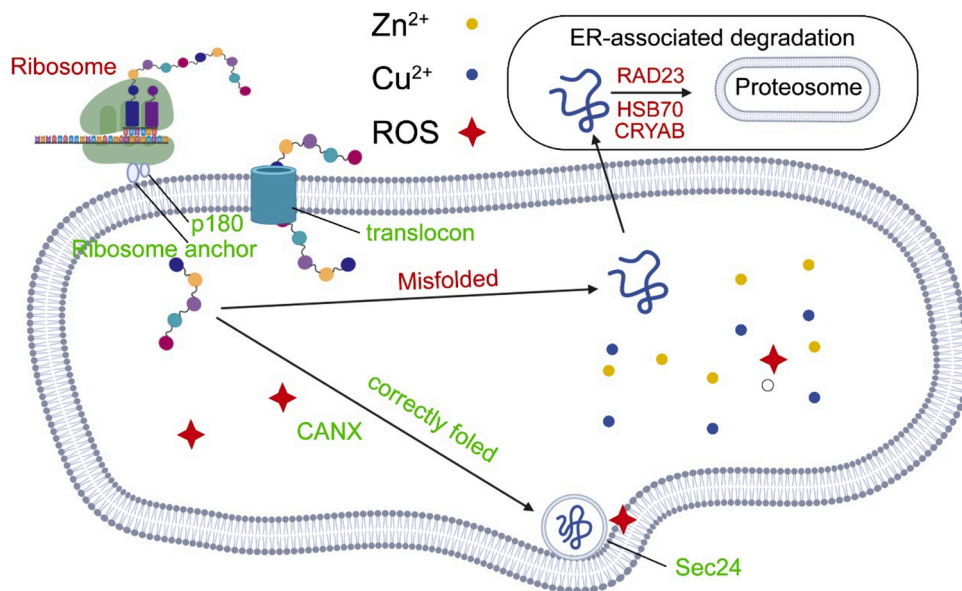


Fig. 6. The altered translation derived from the metal stress (Created with Biorender.com). The green color indicates downregulation, and red color indicates upregulation. CANX: calnexin, CRYAB: alpha-crystallin B chain, HSP70: heat shock protein 70, p180: Ribosome-binding protein 1, RAD23: UV excision repair protein RAD23, Sec24: Protein transport protein Sec24. Created with bioRender.com.

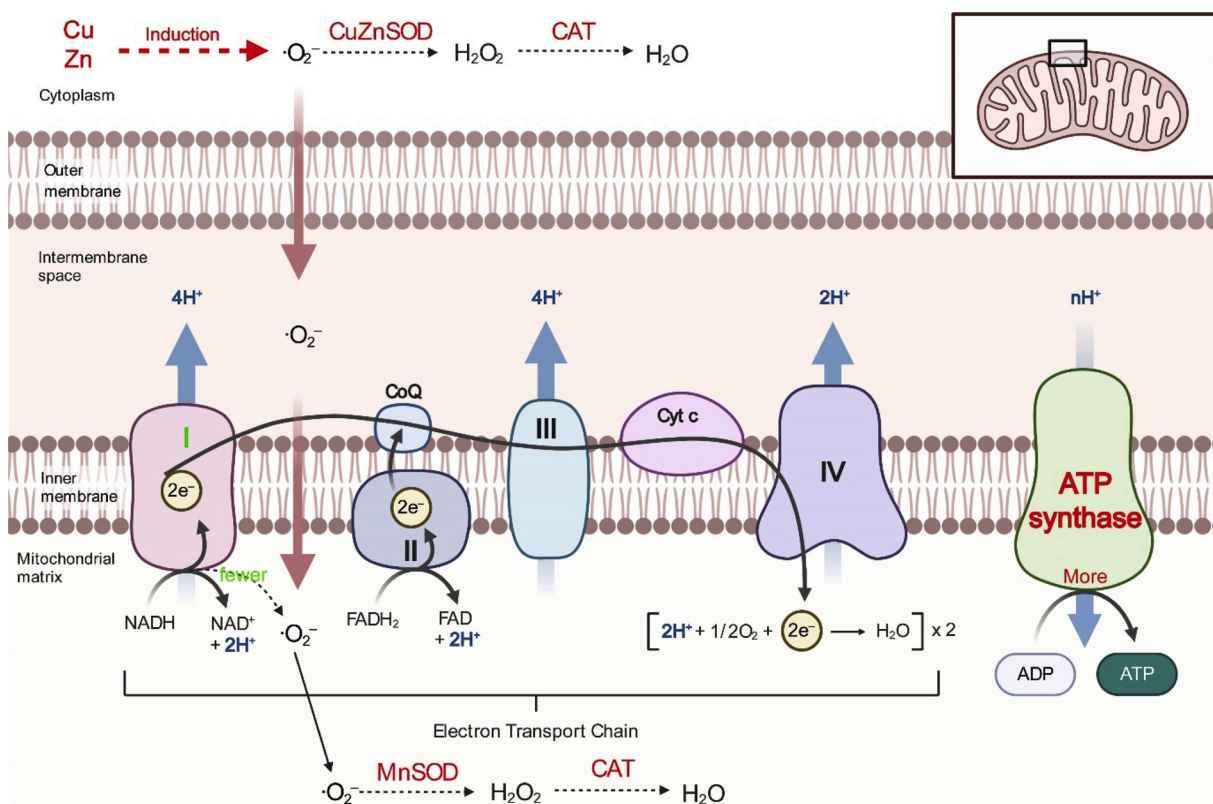


Fig. 7. The proposed process to ROS toxicity in Cu/Zn accumulated oysters (Created with Biorender.com). CAT: Catalase, MnSOD: Mn Superoxide dismutase, CuZnSOD: Cu/Zn Superoxide dismutase. The green color indicates downregulation, and red color indicates upregulation or higher level compared to Site 1. Created with bioRender.com.

this study, higher ROS production was prevalent in severely contaminated oysters (Site 3), as inferred by the elevated activities of antioxidant enzymes.

As a strategy to cope with the stress, the activity of complex I was reduced with signifying lower endogenous ROS production. Two subunits of complex I were significantly lower (0.61-0.81-fold) in oysters

from Site 3 than those at Site 1, indicating a less efficient or damaged complex I. When NADH is transformed into NAD⁺ in complex I, superoxide is produced simultaneously. Dysfunction of complex I thus leads to less ROS production. However, less capability of electron transfer chain might induce dysfunctional energy production in oxidative phosphorylation. To maintain the homeostasis, higher activity of

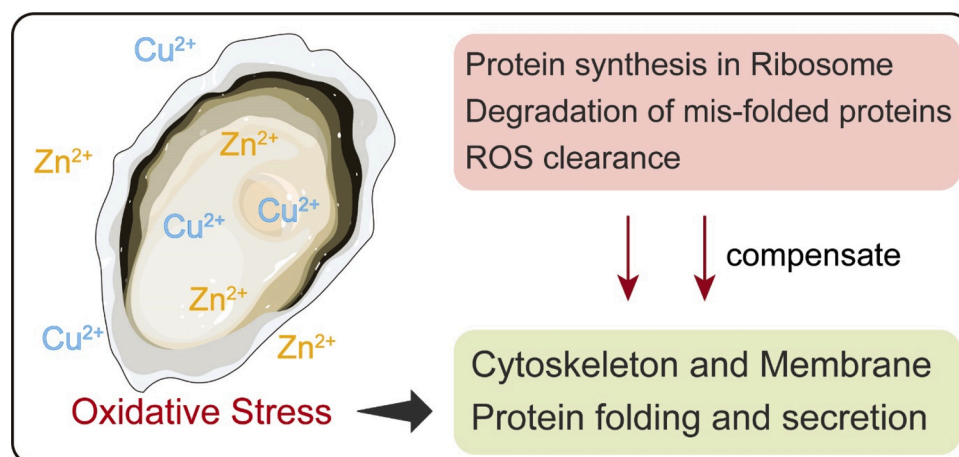


Fig. 8. The overall response to high Cu and Zn body burden at the protein level. Generally, the accumulated Cu and Zn induced the ROS, which threatened the cytoskeleton and membrane trafficking, and protein folding and secretion. Oysters tried to enhance the protein synthesis in ribosome, degradation of mis-folded proteins, and the ROS clearance to compensate for those damage. Red frame signifies elevated functions whereas green frames signifies the downregulated functions.

Table 1

The expression change of antioxidant enzymes, referring to the proteome analysis from iTRAQ. Red color means that the corresponding protein was expressed higher than that of control with statistical significance.

	Site 2	Site 3
alpha-crystallin B chain	1.18	1.23
heat shock protein 70 B2	1.13	1.68
stress-70 protein, mitochondrial	1.14	1.19
catalase	0.88	1.15
glutathione S-transferase Y1-like	0.71	1.19
glutathione S-transferase omega-1-like	0.83	1.16
superoxide dismutase [Mn], mitochondrial	0.86	1.19
superoxide dismutase [Cu-Zn]	0.89	2.10

ATP synthase can supply enough energy in responding to metal stress, with the higher abundance of ATP synthase subunit delta (1.17-fold at Site 3).

Furthermore, the activity of downstream ROS detoxification also increased as indicated by the "Longevity regulating pathway" (Fig. 3B). iTRAQ results showed higher activities of antioxidants in oysters from Site 3. SODs and CAT are the active enzymes transforming and detoxifying ROS (Fig. 7). Specifically, superoxide is transformed into H_2O_2 with the help of SODs and then degraded into O_2 and H_2O with the catalysis of CAT. In the severely contaminated oysters, the enhanced activities of these enzymes indicate the possible molecular mechanisms why oysters are able to survive in metal contaminated estuaries: ROS is induced by excess Cu and Zn in the cytoplasm and extracellular region (Fig. 7). The enhanced superoxide dismutase [Cu-Zn] (CuZnSOD, 2.10-fold at Site 3, Fig. 5E) helps to transform the O_2^- to H_2O_2 in cytoplasm more efficiently. On the other hand, there would be a higher level of O_2^- in mitochondria although oysters reduced the ROS production by NADH dehydrogenase actively, since the ROS induced by Cu and Zn could penetrate mitochondria membranes (Fig. 7). The higher abundance of manganese SOD (MnSOD) in mitochondria is associated with the higher ROS (Figs. 5D and 8). However, the H_2O_2 generated from the reaction by SODs could still pose a threat to their targets (DNA, protein, and lipid). In this study, oysters under severe metal contamination tended to detoxify H_2O_2 into O_2 and H_2O with the help of catalase (CAT, 1.15-fold, Fig. 5F) (Fig. 7).

Oysters are likely to experience severe oxidative stress induced by excess Cu and Zn ions during field and long-term exposure, which might cause dysfunction and affect the homeostasis of protein. Apart from the enhanced ability to translate mRNA in the ribosome and degrade

misfolded proteins, it is more efficient to reduce the total amount of ROS. In the present study, oysters biochemically adapted to severely metal contaminated environments. There was a certain level of tolerance to oxidative stress in oysters when facing a high metal body burden. Overall, CAT and three different types of SODs worked cooperatively to keep the oxidative stress at tolerable levels in oysters, preventing more proteins, DNA and lipids from ROS (Fig. 8).

4. Conclusion

The present study investigated responses at the protein-level to exposure to Cu and Zn in field-collected oysters (*C. hongkongensis*), comparing specimens with more than 50-fold differences in metals. Oysters with the highest body burdens of Cu and Zn, collected at the most contaminated site, showed significantly altered protein expression patterns, compared to oysters with lower body burdens, indicating a positive correlation between the number of DEPs and metal accumulation. Unlike the traditional biochemical markers, proteomics can be a unique tool to study the functional alteration and assess the health risk on oysters under metal accumulation. Due to hyper-accumulated metals, high oxidative stress resulted in damage to some structural proteins of the cytoskeleton and some proteins related to membrane tracking. In addition to the elevated expression of ribosome-associated metals, there was higher activity of proteins participating in the degradation of mis-folded or impaired proteins by metals indirectly or directly. Furthermore, a lower expression of ROS generated enzyme (NADH dehydrogenase) and a greater expression of ROS-scavengers (SODs and CAT) was observed to reduce the damage (Fig. 8). This study corroborated the change of protein profile in oysters under different levels of Cu/Zn accumulation in the estuaries, providing more insights into the responses to metals and the underlying mechanism at the protein level. Finally, it is also important to further explore the integrated effects of organic pollutants and other physical-chemical parameters on proteomic profiles.

CRediT authorship contribution statement

Yunlong Li: Conceptualization, Investigation, Writing - review & editing. **Wen-Xiong Wang:** Conceptualization, Writing - review & editing.

Declaration of Competing Interest

The authors declare that they have no known competing financial

interests or personal relationships that could have appeared to influence the work reported in this paper.

Acknowledgements

We thank the two anonymous reviewers for their comments. This study was supported by the Natural Science Foundation of China (21777134), the General Research Fund of Hong Kong Research Grants Council (CityU 16102918), the TUYF fund (19SC01), and the Hong Kong Branch of Southern Marine Science and Engineering Guangdong Laboratory (Guangzhou) (SMSEGL20SC01).

Appendix A. Supplementary data

Supplementary material related to this article can be found, in the online version, at doi:<https://doi.org/10.1016/j.aquatox.2021.105749>.

References

- Abdal Dayem, A., Hossain, M.K., Lee, S.B., Kim, K., Saha, S.K., Yang, G.-M., Choi, H.Y., Cho, S.-G., 2017. The role of reactive oxygen species (ROS) in the biological activities of metallic nanoparticles. *Int. J. Mol. Sci.* 18, 120.
- Adele, D.J., Wei, W., Smith, N., Bies, J.J., Lee, J., 2009. Cadmium-mediated rescue from ER-associated degradation induces expression of its exporter. *Proc. Natl. Acad. Sci.* 106, 10189.
- Auten, R.L., Davis, J.M., 2009. Oxygen toxicity and reactive oxygen species: the devil is in the details. *Pediatr. Res.* 66, 121–127.
- Bao, Y., Liu, X., Zhang, W., Cao, J., Li, W., Li, C., Lin, Z., 2016. Identification of a regulation network in response to cadmium toxicity using blood clam *Tegillarca granosa* as model. *Sci. Rep.* 6, 35704.
- Barber-Zucker, S., Shaan, B., Zarivach, R., 2017. Transition metal binding selectivity in proteins and its correlation with the phylogenomic classification of the cation diffusion facilitator protein family. *Sci. Rep.* 7, 16381.
- Bejaoui, S., Michán, C., Telahigue, K., Nechi, S., Cafsi, Me., Soudani, N., Blasco, J., Costa, P.M., Alhama, J., 2020. Metal body burden and tissue oxidative status in the bivalve *Venerupis decussata* from Tunisian coastal lagoons. *Mar. Environ. Res.* 159, 105000.
- Camacho, C., Coulouris, G., Avagyan, V., Ma, N., Papadopoulos, J., Bealer, K., Madden, T.L., 2009. BLAST+: architecture and applications. *BMC Bioinformatics* 10, 421.
- Ceresa, B.P., Schmid, S.L., 2000. Regulation of signal transduction by endocytosis. *Curr. Opin. Cell Biol.* 12, 204–210.
- Chan, C.Y., Wang, W.-X., 2018a. A lipidomic approach to understand copper resilience in oyster *Crassostrea hongkongensis*. *Aquat. Toxicol.* 204, 160–170.
- Chan, C.Y., Wang, W.-X., 2018b. Seasonal and spatial variations of biomarker responses of rock oysters in a coastal environment influenced by large estuary input. *Environ. Pollut.* 242, 1253–1265.
- Chan, C.Y., Wang, W.-X., 2019. Biomarker responses in oysters *Crassostrea hongkongensis* in relation to metal contamination patterns in the Pearl River Estuary, Southern China. *Environ. Pollut.* 251, 264–276.
- Chen, C., Chen, H., Zhang, Y., Thomas, H.R., Frank, M.H., He, Y., Xia, R., 2020. TBtools: an integrative toolkit developed for interactive analyses of big biological data. *Mol. Plant* 13, 1194–1202.
- Cho, W., Stahelin, R.V., 2005. Membrane-protein interactions in cell signaling and membrane trafficking. *Annu. Rev. Biophys. Biomol. Struct.* 34, 119–151.
- de la Cruz, J., Karbstein, K., Woolford Jr, J.L., 2015. Functions of ribosomal proteins in assembly of eukaryotic ribosomes in vivo. *Annual Reviews of Biochemistry* 84, 93–129.
- Deutsch, E.W., Mendoza, L., Shteynberg, D., Farrah, T., Lam, H., Tasman, N., Sun, Z., Nilsson, E., Pratt, B., Prazen, B., Eng, J.K., Martin, D.B., Nesvizhskii, A.I., Aebersold, R., 2010. A guided tour of the Trans-Proteomic Pipeline. *Proteomics* 10, 1150–1159.
- Di, C., Syafrizayanti, Zhang, Q., Chen, Y., Wang, Y., Zhang, X., Liu, Y., Sun, C., Zhang, H., Hoheisel, J.D., 2019. Function, clinical application, and strategies of Pre-mRNA splicing in cancer. *Cell Death Differ.* 26, 1181–1194.
- Dineshram, R., Quan, Q., Sharma, R., Chandramouli, K., Yalamanchili, H.K., Chu, I., Thiagarajan, V., 2015. Comparative and quantitative proteomics reveal the adaptive strategies of oyster larvae to ocean acidification. *Proteomics* 15, 4120–4134.
- Eng, J.K., Jahan, T.A., Hoopmann, M.R., 2013. Comet: an open-source MS/MS sequence database search tool. *Proteomics* 13, 22–24.
- Faini, M., Beck, R., Wieland, F.T., Briggs, J.A.G., 2013. Vesicle coats: structure, function, and general principles of assembly. *Trends Cell Biol.* 23, 279–288.
- Giarratano, E., Duarte, C.A., Amin, O.A., 2010. Biomarkers and heavy metal bioaccumulation in mussels transplanted to coastal waters of the Beagle Channel. *Ecotoxicol. Environ. Saf.* 73, 270–279.
- Gu, Y.-G., Ke, C.-L., Gao, Y.-P., Liu, Q., Li, Y.-F., 2020. Nonmetric multidimensional scaling and adverse effects on aquatic biota of polycyclic aromatic hydrocarbons in sediments: A case study of a typical aquaculture wetland, China. *Environ. Res.* 182, 109119.
- Han, D., Currell, M.J., 2017. Persistent organic pollutants in China's surface water systems. *Sci. Total Environ.* 580, 602–625.
- Herrmann, J.M., Spang, A., 2015. Intracellular parcel service: current issues in intracellular membrane trafficking. In: Tang, B.L. (Ed.), *Membrane Trafficking*, second edition. Springer New York, New York, NY, pp. 1–12.
- Ji, C., Wang, Q., Wu, H., Tan, Q., Wang, W.-X., 2015. A metabolomic investigation of the effects of metal pollution in oysters *Crassostrea hongkongensis*. *Mar. Pollut. Bull.* 90, 317–322.
- Kaiser, D., Hand, I., DanielaUnger, Schulz-Bull, D.E., Waniek, J.J., 2015. Organic pollutants in the central and coastal Beibu Gulf, South China Sea. *Mar. Pollut. Bull.* 101, 972–985.
- Kammers, K., Cole, R.N., Tiengwe, C., Ruczninski, I., 2015. Detecting significant changes in protein abundance. *EuPA Open Proteom.* 7, 11–19.
- Kanehisa, M., Sato, Y., Morishima, K., 2016. BlastKOALA and GhostKOALA: KEGG Tools for functional characterization of genome and metagenome sequences. *J. Mol. Biol.* 428, 726–731.
- Katerji, M., Filippova, M., Duerksen-Hughes, P., 2019. Approaches and methods to measure oxidative stress in clinical samples: research applications in the cancer field. *Oxid. Med. Cell. Longev.* 2019, 1279250.
- Kaur, P., Rizk, N.M., Ibrahim, S., Younes, N., Uppal, A., Dennis, K., Karve, T., Blakeslee, K., Kwagyan, J., Zirie, M., Resson, H.W., Cheema, A.K., 2012. iTRAQ-Based Quantitative protein expression profiling and MRM verification of markers in Type 2 diabetes. *J. Proteome Res.* 11, 5527–5539.
- Khalil, A.M., 2015. Toxicological effects and oxidative stress responses in freshwater snail, *Lanistes carinatus*, following exposure to chlorpyrifos. *Ecotoxicol. Environ. Saf.* 116, 137–142.
- Klimova, Y.S., Chuiko, G.M., Gapeeva, M.V., Pesnya, D.S., Ivanova, E.I., 2019. The use of oxidative stress parameters of bivalve mollusks *Dreissena polymorpha* (Pallas, 1771) as biomarkers for ecotoxicological assessment of environment. *Inland Water Biol.* 12, 88–95.
- Li, Y., Wang, Z., Zhao, Z., Cui, Y., 2019. iTRAQ-based proteome profiling of hyposaline responses in zygotes of the Pacific oyster *Crassostrea gigas*. *Comp. Biochem. Physiol. Part D Genomics Proteomics* 30, 14–24.
- Li, Y., Zhang, X., Meng, J., Chen, J., You, X., Shi, Q., Wang, W.-X., 2020. Molecular responses of an estuarine oyster to multiple metal contamination in Southern China revealed by RNA-seq. *Sci. Total Environ.* 701, 134648.
- Liao, Q., Zhao, L., Chen, X., Deng, Y., Ding, Y., 2008. Serum proteome analysis for profiling protein markers associated with carcinogenesis and lymph node metastasis in nasopharyngeal carcinoma. *Clin. Exp. Metastasis* 25, 465–476.
- Lin, L.-S., Wang, J.-F., Song, J., Liu, Y., Zhu, G., Dai, Y., Shen, Z., Tian, R., Song, J., Wang, Z., Tang, W., Yu, G., Zhou, Z., Yang, Z., Huang, T., Niu, G., Yang, H.-H., Chen, Z.-Y., Chen, X., 2019. Cooperation of endogenous and exogenous reactive oxygen species induced by zinc peroxide nanoparticles to enhance oxidative stress-based cancer therapy. *Theranostics* 9, 7200–7209.
- Liu, F., Wang, W.-X., 2012. Proteome pattern in oysters as a diagnostic tool for metal pollution. *J. Hazard. Mater.* 239–240, 241–248.
- Liu, X., Wang, W.-X., 2016a. Antioxidant and detoxification responses of oysters *Crassostrea hongkongensis* in a multimetal-contaminated estuary. *Environ. Toxicol. Chem.* 35, 2798–2805.
- Liu, X., Wang, W.-X., 2016b. Physiological and cellular responses of oysters (*Crassostrea hongkongensis*) in a multimetal-contaminated estuary. *Environ. Toxicol. Chem.* 35, 2577–2586.
- Liu, X., Wang, W.-X., 2016c. Time changes in biomarker responses in two species of oyster transplanted into a metal contaminated estuary. *Sci. Total Environ.* 544, 281–290.
- Long, E.R., Macdonald, D.D., Smith, S.L., Calder, F.D., 1995. Incidence of adverse biological effects within ranges of chemical concentrations in marine and estuarine sediments. *Environ. Manage.* 19, 81–97.
- Lu, G.-Y., Ke, C.-H., Zhu, A., Wang, W.-X., 2017. Oyster-based national mapping of trace metals pollution in the Chinese coastal waters. *Environ. Pollut.* 224, 658–669.
- Lu, G., Zhu, A., Fang, H., Dong, Y., Wang, W.-X., 2019a. Establishing baseline trace metals in marine bivalves in China and worldwide: meta-analysis and modeling approach. *Sci. Total Environ.* 669, 746–753.
- Lu, Z., Shan, X., Ji, C., Zhao, J., Wu, H., 2019b. Proteomic responses induced by metal pollutants in oysters *Crassostrea sikamea*. *J. Oceanol. Limnol.* 37, 685–693.
- Luo, L., Ke, C., Guo, X., Shi, B., Huang, M., 2014. Metal accumulation and differentially expressed proteins in gill of oyster (*Crassostrea hongkongensis*) exposed to long-term heavy metal-contaminated estuary. *Fish Shellfish Immunol.* 38, 318–329.
- Marrocco, I., Altieri, F., Peluso, I., 2017. Measurement and clinical significance of biomarkers of oxidative stress in humans. *Oxid. Med. Cell. Longev.* 2017, 6501046.
- Masood, M., Raftos, D.A., Nair, S.V., 2016. Two oyster species that show differential susceptibility to virus infection also show differential proteomic responses to generic dsRNA. *J. Proteome Res.* 15, 1735–1746.
- Mateer, S.C., Wang, N., Bloom, G.S., 2003. IQGAPs: integrators of the cytoskeleton, cell adhesion machinery, and signaling networks. *Cell Motil.* 55, 147–155.
- Meng, J., Wang, W.-X., Li, L., Zhang, G., 2017a. Respiration disruption and detoxification at the protein expression levels in the Pacific oyster (*Crassostrea gigas*) under zinc exposure. *Aquat. Toxicol.* 191, 34–41.
- Meng, J., Wang, W., Li, L., Yin, Q., Zhang, G., 2017b. Cadmium effects on DNA and protein metabolism in oyster (*Crassostrea gigas*) revealed by proteomic analyses. *Sci. Rep.* 7, 11716.
- Meng, J., Wang, W.-X., Li, L., Zhang, G., 2018. Tissue-specific molecular and cellular toxicity of Pb in the oyster (*Crassostrea gigas*): mRNA expression and physiological studies. *Aquat. Toxicol.* 198, 257–268.

- Mesquita, A.F., Marques, S.M., Marques, J.C., Gonçalves, F.J.M., Gonçalves, A.M.M., 2019. Copper sulphate impact on the antioxidant defence system of the marine bivalves *Cerastoderma edule* and *Scrobicularia plana*. *Sci. Rep.* 9, 16458.
- Muralidharan, S., Thompson, E., Raftos, D., Birch, G., Haynes, P.A., 2012. Quantitative proteomics of heavy metal stress responses in Sydney rock oysters. *PROTEOMICS* 12, 906–921.
- Murphy, M.P., 2009. How mitochondria produce reactive oxygen species. *Biochem. J.* 417, 1–13.
- Nesvizhskii, A.I., Keller, A., Kolker, E., Aebersold, R., 2003. A statistical model for identifying proteins by tandem mass spectrometry. *Anal. Chem.* 75, 4646–4658.
- O'Brien, J., Hayder, H., Zayed, Y., Peng, C., 2018. Overview of MicroRNA biogenesis, mechanisms of actions, and circulation. *Front. Endocrinol. (Lausanne)* 9, 402.
- Pan, K., Wang, W.-X., 2012. Trace metal contamination in estuarine and coastal environments in China. *Sci. Total Environ.* 421–422, 3–16.
- Pfeffer, S., Burbaum, L., Unverdorben, P., Pech, M., Chen, Y., Zimmermann, R., Beckmann, R., Förster, F., 2015. Structure of the native Sec61 protein-conducting channel. *Nat. Commun.* 6, 8403.
- Podgurskaya, O.V., Kavun, V.Y., 2006. Subcellular distribution of heavy metals in organs of bivalvemodiolus modiolus living along a metal contamination gradient. *Ocean. Sci. J.* 41, 43–51.
- Qiao, Y., Yang, Y., Zhao, J., Tao, R., Xu, R., 2013. Influence of urbanization and industrialization on metal enrichment of sediment cores from Shantou Bay, South China. *Environ. Pollut.* 182, 28–36.
- Song, X., Bandow, J., Sherman, J., Baker, J.D., Brown, P.W., McDowell, M.T., Molloy, M.P., 2008. iTRAQ experimental design for plasma biomarker discovery. *J. Proteome Res.* 7, 2952–2958.
- Stadtman, E.R., Levine, R.L., 2000. Protein oxidation. *Ann. N. Y. Acad. Sci.* 899, 191–208.
- Su, W., Rong, J., Zha, S., Yan, M., Fang, J., Liu, G., 2018. Ocean acidification affects the cytoskeleton, lysozymes, and nitric oxide of hemocytes: a possible explanation for the hampered phagocytosis in blood clams, *Tegillarca granosa*. *Front. Physiol.* 9, 619.
- Sun, Z., Brodsky, J.L., 2017. Guardians of the ERAD galaxy. *Cell* 171, 267–268.
- Tan, Q.-G., Wang, Y., Wang, W.-X., 2015. Speciation of Cu and Zn in two colored oyster species determined by x-ray absorption spectroscopy. *Environ. Sci. Technol.* 49, 6919–6925.
- Thompson, E.L., Taylor, D.A., Nair, S.V., Birch, G., Haynes, P.A., Raftos, D.A., 2012. Proteomic discovery of biomarkers of metal contamination in Sydney Rock oysters (*Saccostrea glomerata*). *Aquat. Toxicol.* 109, 202–212.
- Tian, Y., Liu, H., Zheng, T., Kwon, K., Kim, S., Yan, C., 2008. PAHs contamination and bacterial communities in mangrove surface sediments of the Jiulong River Estuary, China. *Mar. Pollut. Bull.* 57 (6–12), 707–715.
- Venkataraman, Y.R., Timmins-Schiffman, E., Horwith, M.J., Lowe, A.T., Nunn, B., Vadopalas, B., Spencer, L.H., Roberts, S.B., 2019. Characterization of Pacific oyster *Crassostrea gigas* proteomic response to natural environmental differences. *Mar. Ecol. Prog. Ser.* 610, 65–81.
- Vranković, J., 2015. Environmental impact on the antioxidant responses in *Corbicula fluminea* (Bivalvia: veneroida: corbiculidae) from the Danube River. *Ital. J. Zool. (Modena)* 82, 1–9.
- Wade, S.L., Auble, D.T., 2010. The Rad23 ubiquitin receptor, the proteasome and functional specificity in transcriptional control. *Transcription* 1, 22–26.
- Wang, H., Guo, X., 2008. Identification of *Crassostrea ariakensis* and related oysters by multiplex species-specific PCR. *J. Shellfish Res.* 27, 481–487.
- Wang, W.-X., Yang, Y., Guo, X., He, M., Guo, F., Ke, C., 2011. Copper and zinc contamination in oysters: subcellular distribution and detoxification. *Environ. Toxicol. Chem.* 30, 1767–1774.
- Weng, N., Wang, W.-X., 2015. Reproductive responses and detoxification of estuarine oyster *Crassostrea hongkongensis* under metal stress: a seasonal study. *Environ. Sci. Technol.* 49, 3119–3127.
- Weng, N., Wang, W.-X., 2019. Seasonal fluctuations of metal bioaccumulation and reproductive health of local oyster populations in a large contaminated estuary. *Environ. Pollut.* 250, 175–185.
- Weng, N., Jiang, H., Wang, W.-X., 2017. In situ subcellular imaging of copper and zinc in contaminated oysters revealed by nanoscale secondary ion mass spectrometry. *Environ. Sci. Technol.* 51, 14426–14435.
- Xiao, S., Wong, N.-K., Li, J., Lin, Y., Zhang, Y., Ma, H., Mo, R., Zhang, Y., Yu, Z., 2018. Analysis of in situ transcriptomes reveals divergent adaptive response to hyper- and hypo-salinity in the Hong Kong oyster, *Crassostrea hongkongensis*. *Front. Physiol.* 9, 1491.
- Xu, L., Ji, C., Wu, H., Tan, Q., Wang, W.-X., 2016. A comparative proteomic study on the effects of metal pollution in oysters *Crassostrea hongkongensis*. *Mar. Pollut. Bull.* 112, 436–442.
- Xu, J., Wise, J.T.F., Wang, L., Schumann, K., Zhang, Z., Shi, X., 2017. Dual roles of oxidative stress in metal carcinogenesis. *Journal of Environmental Pathology, Toxicology and Oncology* 36, 345–376.
- Xu, J., Zheng, L., Xu, L., Liu, B., Liu, J., Wang, X., 2020. Identification of dissolved metal contamination of major rivers in the southeastern hilly area, China: distribution, source apportionment, and health risk assessment. *Environ. Sci. Pollut. Res. - Int.* 27, 3908–3922.
- Yamamoto, S., Yamashita, A., Arakaki, N., Nemoto, H., Yamazaki, T., 2014. Prevention of aberrant protein aggregation by anchoring the molecular chaperone α B-crystallin to the endoplasmic reticulum. *Biochem. Biophys. Res. Commun.* 455, 241–245.
- Yan, L.-R., Wang, D.-X., Liu, H., Zhang, X.-X., Zhao, H., Hua, L., Xu, P., Li, Y.-S., 2014. A pro-atherogenic HDL profile in coronary heart disease patients: an iTRAQ labelling-based proteomic approach. *PLoS One* 9, e98368.
- Young, M.D., Wakefield, M.J., Smyth, G.K., Oshlack, A., 2010. Gene ontology analysis for RNA-seq: accounting for selection bias. *Genome Biol.* 11, R14.
- Yu, X.-J., Pan, K., Liu, F., Yan, Y., Wang, W.-X., 2013. Spatial variation and subcellular binding of metals in oysters from a large estuary in China. *Mar. Pollut. Bull.* 70, 274–280.
- Zhang, Y., Sun, J., Mu, H., Li, J., Zhang, Y., Xu, F., Xiang, Z., Qian, P.-Y., Qiu, J.-W., Yu, Z., 2015. Proteomic basis of stress responses in the gills of the Pacific oyster *Crassostrea gigas*. *J. Proteome Res.* 14, 304–317.
- Zhao, X., Yu, H., Kong, L., Li, Q., 2012. Transcriptomic responses to salinity stress in the Pacific oyster *Crassostrea gigas*. *PLoS One* 7, e46244.